Talanta xxx (xxxx) xxx

Contents lists available at ScienceDirect

Talanta

journal homepage: www.elsevier.com/locate/talanta

Aptamer selection and aptasensor construction for bone density biomarkers

Raja Chinnappan [a], Norhan Sameh Zaghloul [b], Razan AlZabn [a], Abeer Malkawi [c], Anas Abdel Rahman [c,d,e], Khalid M. Abu-Salah [b], Mohammed Zourob [a,d,*]

[a] Department of Chemistry, Alfaisal University, Al Zahrawi Street, Al Maather, Al Takhassusi Rd, Riyadh, 11533, Saudi Arabia
[b] Department of Cellular Therapy and Cancer Research-Nanomedicine Section, King Abdullah International Medical Research Center/ King Saud Bin Abdulaziz University for Health Sciences, Ministry of the National Guard-Health Affairs, Riyadh, Saudi Arabia
[c] Department of Genetics, Research Center, King Faisal Specialist Hospital and Research Center, Zahrawi Street, Al Maather, Riyadh, 12713, Saudi Arabia
[d] Department of Biochemistry and Molecular Medicine, College of Medicine, Alfaisal University, Riyadh, Saudi Arabia
[e] Department of Chemistry, College of Science, Memorial University of Newfoundland, St. JOhn's, NL, A1B 3X7, Canada

ARTICLE INFO

Keywords:
Osteoporosis
Osteocalcin
Beta-crosslap
Graphene-oxide
Aptamer
Biosensor
Aptasensor
FRET

ABSTRACT

Osteoporosis (OP) is a bone disease involved in dysregulation of one of the bone metabolism arms, formation, or desorption cause a porous bone. Osteocalcin (OC) and beta-crosslap (BC), are the well-known markers for OP, which are connected to bone formation and desorption, respectively. In addition to the OP biomarker, BC is also used as an estrogen replacement therapeutic monitoring. ELISA and other antibody-based detection methods are routinely used for measuring OC and BC. These methods have limitations that include thermostability, sensitivity, sacrificing animals, and cost of production. However, aptamer-based-assays are of interest to overcome these drawbacks and achieve the most specific and robust application. Herein, specific aptamers for OC and BC were selected by the systematic evolution of ligands by exponential enrichment (SELEX) method from the pool of ssDNA library with 60 random sequences. The binding affinity (K_d) of the selected aptamers were evaluated against the respective biomarkers. The high-affinity aptamers of OC and BC showed the K_d values of 59 and 55 nM respectively. A graphene oxide-based aptasensors were fabricated from the high-affinity aptamers, and the detection limits of OC and BC were found to be 0.4 pg/ml and 0.21 pg/ml, respectively. These aptasensors have been tested with OC and BC spiked buffer samples and validated using serum samples collected from osteoporotic rats.

1. Introduction

Osteoporosis (OP) is a progressive metabolic and skeletal disease, portrayed by a decrease in bone mass, bone mineral density (BMD), and deterioration in the microarchitecture of bone tissue, which leads to an increase in the susceptibility to bone fracture and fragility [1]. OP is a prevalent health issue, primarily for the aging population. Every year, about 54 million women and men are diagnosed with OP worldwide, two million of whom develop osteoporosis-related fractures [2]. The three most essential fragility fractures associated with OP are hip, spine, and wrist [3]. Moreover, 10–20% of hip fractures lead to death during the first year of incidence [4]. The prevalence of OP among the Saudi population range from 35 to 48% [5]. The economic cost regarding OP management and its related fractures is $12.78 million annually in Saudi Arabia [6]. Dual Energy Absorptiometry (DXA) has become a gold standard tool for measuring BMD and confirm the diagnosis for OP using a t-score. Based on DXA, patients with t-score $\leq$ 2.5 and 2.5 - 1 are diagnosed with OP and osteopenia (ON), respectively [7]. Several risk factors play a critical role in OP development, including genetics and age. Bone turnover markers change with aging fracture history [2,8]. Chronic disease conditions, such as diabetes, possess low BMD and high risk of fragility fracture [9]. However, moderate physical activity has an enhancement effect on bone density [10]. Body mass index (BMI) is considered as a complicated factor, where low BMI counts as a risk factor for hip fractures and a protective factor for lower leg fractures [11]. Various drugs decrease the risk of bone fractures, including estrogen replacement therapy, selective estrogen receptor modulators (SERM), and calcitonin [12]. Calcium, vitamin D and vitamin K2 supplementation have been found to influence bone formation [13]. However, several medications have been reported to decrease BMD and elevate fracture incidence such as glucocorticoids that stimulate bone resorption and decrease bone formation [14].

* Corresponding author. Department of Chemistry, Alfaisal University, Al Zahrawi Street, Al Maather, Al Takhassusi Rd, Riyadh, 11533, Saudi Arabia.
E-mail address: mzourob@alfaisal.edu (M. Zourob).

https://doi.org/10.1016/j.talanta.2020.121818
Received 16 August 2020; Received in revised form 23 October 2020; Accepted 26 October 2020
Available online 29 October 2020
0039-9140/

Osteocalcin (OC) is a 49 amino acid long protein, secreted by osteoblasts and considered one of the abundant non-collagenous proteins, also known as Gla protein. Osteocalcin (OC) is known as a bone formation biomarker that has a role in bone mineralization due to its ability to bind with calcium and helps in the differentiation of osteoblast. Changes in OC serum level indicate a bone turnover, where the level reduction in serum indicates a loss in bone formation [15]. Alkaline phosphatase (ALP) is another bone remodeling biomarker that is considered a non-specific biomarker for the bone disorder because, different isoforms are produced by various tissues [16]. A reduction in ALP is found when bone formation is reduced by inhibiting the activity of osteoblast [17], while a high level of ALP indicates an enhancement in bone resorption [18]. ß-Carboxy-Terminal Cross-Linking Telopeptide of Type I Collagen; (ß-CrossLaps, ß-CTX) is a specific bone resorption biomarker that is released to circulation during the degradation of collagen type-1 in bone [19]. An elevation in β-crosslaps serum level indicates bone resorption enhancement.

OC analysis in biological fluids is very challenging, mainly in mass spectrometry due to the multiple carboxylations at glutamic residues [20]. The glutamic residues usually bind to metal ions, which reduces the ionization using electron spray ionization (ESI). Immunological methods are the most available and useful techniques for measuring the OC in the biological matrices. Recently, a porous silicon competitive ELISA was developed with a significant improvement in detection [21] compared to previous methods [22].

The beta-crosslap level in serum is mainly measured as a C-terminal telopeptide of type I collagen, which is the most reliable serum marker for bone resorption and estrogen replacement therapeutic monitoring. Mainly, beta-crosslaps is analyzed using an immunoreactivity-based technique such as Electrochemiluminescence Immunoassay [23], ELISA [24,25]. These immunoassays have drawbacks associated with the antibody. Its cross-reactivity, sensitivity to the matrix, and sample interference are the major considerations that affect the analyte signal in these assays.

Aptamers are single-strand DNA or RNA which can fold into unique complexed three-dimensional structures and bind to the target analytes with high specificities and affinities [26–31]. The specific aptamers are usually selected from a library of 10^{12}-10^{15} oligonucleotide sequences through a SELEX process (Systematic Evolution of Ligands by Exponential Enrichment). The running cost, easy to produce, chemically stable, size and flexibility to be chemically modified makes these aptasensors are an ideal tool to be translated to clinical laboratories. The aptamer can bind to its target with high selectivity, affinity, and specificity. The specific aptamers have been proven to bind with high affinity to small molecules [26,27,32–34]. Therefore, they are considered as a valid alternative to antibodies for biosensors development. The number of nucleotides in the aptamer varies between 40 and 100, which form suitable unique secondary or tertiary structures and bind to their target with high-affinity stable complex.

Herein, we introduce a biosensor-based method that measures the levels of OC and BC in rat serum using specific aptamers. Specific aptamers against BC and OC were obtained after twelve rounds of selection, and the dissociation constants of each analyte show in sub-nanomolar levels. Aptamer based biosensors for these two analytes have been developed by fluorescence ON/OFF switching mechanism (Scheme 1). These methods were validated by spiking the analytes in the buffer, and the percentage recovery was very close with the spiked amount. Finally, we estimate the amount of BC and OC in known serum samples. As this is very simple and fast, we believe that these sensors might be applied for the analysis of clinical samples.

2. Experimental

2.1. Materials and reagents

The target analyte, Rat osteocalcin (OC) was obtained from

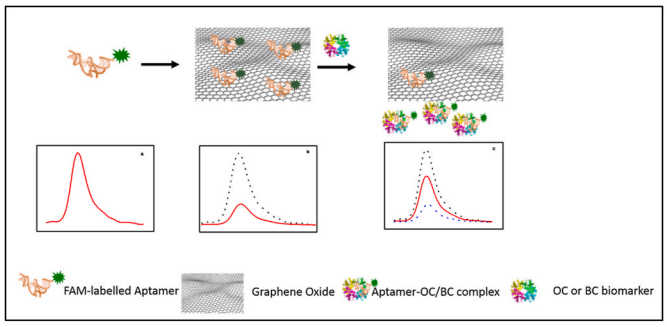

Scheme 1. Schematic diagram of graphene oxide aptasensor working principle using BC and OC specific aptamers.

Elabscience (Houston, TX USA; www.elabscience.com). Rat beta-Crosslaps was supplied by Abbexa Ltd (Cambridge, UK; https://www.abbexa.com/). N-hydroxysuccinimide (NHS) activated sepharose-4B was purchased from GE Healthcare (Milwaukee, WI, USA; https://www.gelifesciences.com). PBS buffer tablets, sodium chloride (NaCl), magnesium chloride ($MgCl_2$), phosphate-buffered saline pH 7.4 (PBS), *tris*(hydroxymethyl)aminomethane (tris-base), boric acid, ethylenediaminetetraacetic acid (EDTA) disodium dehydrate, acrylamide/bisacrylamide (30% solution), tetramethylethylenediamine (TEMED), urea, ammonium persulfate (APS), sodium acetate, sodium bicarbonate, sodium azide, hydrochloric acid, bovine serum albumin (BSA), sodium carbonate anhydrous, sodium bicarbonate, dipotassium hydrogen orthophosphate, potassium dihydrogen orthophosphate ethanol and N, N-dimethyl formamide (DMF) were all purchased from Sigma-Aldrich (St Louis, MO, USA; https://www.sigmaaldrich.com/united-states.html). Taq buffer, dNTPs, Taq plus polymerase for PCR amplification and 100-base pair ladder were purchased from ACE Biotech (Riyadh, Saudi Arabia). Bromo-4-chloro(3-indolyl-b-D-galactopyranoside, X-Gal was purchased from Bio Basic Inc.(Toronto, ON, Canada; https://www.biobasic.com/). Ampicillin lyophilized powder was purchased from Bio-Rad (Hercules California, USA). The bacteria culture plates were supplied by Saudi Prepared Media Laboratory Company (Riyadh, Saudi Arabia; http://www.spml.com.sa/). For carrying out agarose gel electrophoresis, 50X TAE buffer and agarose powder were procured from Bio-Rad (Hercules, California, United States). Spin-X cellulose acetate centrifuge filter tubes with a pore size of 45 μm were obtained from Corning life sciences (Tewksbury, MA USA; http://www.corning.com). Amicon Ultra Centrifugal Filter (0.5 ml) was obtained from EMD Millipore (Sigma MA USA; https://www.merckmillipore.com). HPLC purified labeled, and unlabeled oligonucleotides and random DNA libraries were purchased from Metabion International (Planegg, Germany; http://www.metabion.com). *E*-coli competent cells and the TOPO TA cloning kit containing the pCR2.1-TOPO vector were bought from Invitrogen Inc. (New York, NY, USA).

For the washing step during the aptamer selection as well as the detection experiments, the binding buffer used was prepared as 2 mM $MgCl_2$, 50 mM Tris (pH 7.5) and 150 mM NaCl in distilled water. For eluting the aptamer sequences bound to the target, elution buffer was used, which is 7 M urea in binding buffer. Tris-EDTA (TE) buffer that was used to elute the ssDNA from the denaturating gel was prepared by mixing 1 mM EDTA and 10 mM Tris (pH 7.4) in distilled water. 0.2 M $NaHCO_3$ (pH 8.3) was used as the coupling buffer for the conjugation of OC and BC with the NHS-activated sepharose beads. 50 mM Tris, pH 8.0, 0.5 M NaCl, and 50 mM sodium acetate pH 4.0, 0.5 M NaCl were used for washing the OC and BC conjugated beads.

2.2. Instrumentation

NanoDrop 2000(Thermo Scientific, Ottawa, Canada)*UV–Vis spectrophotometer* was used to determine the concentration of the DNA and

protein. *Fluorescence* analysis for the fluorescein-labeled aptamers was achieved by using Nanodrop ND3300 fluorospectrometer (Thermo Scientific, Ottawa, Canada). The samples were excited by the light-emitting diodes (LEDs), λ excitation = 470 ± 10 nm, and the emission was monitored at 515 nm. Experiments were performed in triplicate unless otherwise mentioned. All the measurements were recorded in binding buffer (pH, 7.4) at room temperature. The fluorescence spectra are the average of two measurements. The polymerase chain reaction (PCR) was performed in the Bio-Rad T100 Thermal cycler (Hercules, California, USA).

2.3. Preparation of osteocalcin and beta-crosslaps conjugated sepharose beads

Rat osteocalcin (OC) and Rat beta-Crosslaps(BC) were immobilized with carboxylic acid-functionalized sepharose beads activated with N-Hydroxysuccinimide (NHS) for effective coupling with the free amine group in the OC and BC proteins. The sepharose beads were washed with 10–15 vol of 1 mM HCl using Spin-X cellulose acetate centrifuge filter tubes with a pore size of 0.45 μm. The washed beads obtained after centrifugation for 5 min at 600 rpm was treated with target molecules. 100 μg of BC or OC was added to the slurry of the washed sepharose-beads and mixed by the end over end for overnight at 4 °C in coupling buffer (200 mM sodium bicarbonate, pH = 8.3). After conjugation is complete, the filter tubes were centrifuged to remove the liquid and the beads were washed several times with a coupling buffer to remove the unreacted OC or BC. The un-reacted active groups in the beads were quenched by the primary amine of 100 mM Tris buffer (pH = 8.0) for 1 h. The blocked beads were washed six times with 100 mM Tris, 0.5 M NaCl pH = 8.0 and 100 mM sodium acetate, 0.5 M NaCl, pH = 4.0-4.5 alternatively. The washed beads were stored in 10 mM Tris, pH = 7.5, containing 0.02% sodium azide at 4 °C until further use. The same protocol was followed to prepare the blank beads, here Tris-HCl was conjugated with the beads instead of target molecules.

2.4. Library and primer construction

An artificially synthesized random single-strand DNA library (3 nmol ~ 2×10^{15} sequences) was used for the systematic evolution of ligands by exponential enrichment (SELEX) experiments. The polyacrylamide gel electrophoresis (PAGE) purified library consists of a central random region of 60 nucleotides with two fixed regions of 18 nucleotides-sequences at the 3′ and 5′ends. These regions are the primer binding sites for the amplification of the DNA sequences by polymerase chain reaction (PCR). The full-length library is (5′- ATACCAGCTTATTCAATT - N60 -AGATAGTAAGTGCAATCT-3′, 96-mer). To separate the double strand of the PCR product into two single strands, we design a fluorescein-labeled forward primer and a reverse primer, which consists of 18-atom hexa-ethyleneglycol spacer (to block the PCR amplification) followed by 20 A at the end to have a large size of the reverse primer extended DNA strand. The forward primer is: 5′-fluorescein-ATACCAGCTTATTCAATT-3′ and the reverse primer is: 5′-poly dA_{20}-HEGL-AGATTGCACTTACTATCT-3′. The two primer strands with different sizes were separated by denatured polyacrylamide gel electrophoresis. After the completion of SELEX rounds, unlabeled primers were used for PCR amplification before cloning.

In the first round of aptamer selection processes, 3 nmol of ss DNA pool in binding buffer was denatured at 95 °C for 5 min, then immediately cooled for 10 min at 4 °C then incubated at room temperature for 10 min to have maximum complex folded ssDNA. The OC and BC protein-coupled beads incubated with the pretreated DNA library at room temperature for 2 h in Spin-X cellulose acetate centrifuge filter tubes. The unbound ssDNA was removed by washing the beads with 300 μl aliquots of the binding buffer until there is no DNA. The bound DNA was eluted by the addition of 200 μl of hot elution buffer followed by heating at 90 °C for 5 min followed by centrifugation. The bound oligonucleotide was collected and desalted using an ultrafiltration device (Amicon Ultra Centrifugal filter, 3 KDa cut-off filters) by repeated washing with distilled water to remove urea. To follow the target bound ssDNA recovery from each round, the fluorescence of the eluted oligonucleotide was measured from the second round onwards. After seven SELEX rounds, negative/counter selection was carried out by using blank beads in which the NHS activated beads were conjugated with Tris-HCl instead of target molecules. The aptamers pool from the previous round (round 7) was incubated with the blank beads for 2 h. Then the ssDNA from the washes were collected, concentrated, pretreated (heat 95 °C, cool down 4 °C and RT) and then incubated with target conjugated sepharose beads (positive beads) and the normal selection was resumed. PCR amplification was performed for the selected ssDNA pool after each cycle in 23 parallel reaction tubes comprising of 50 μl reaction mixture. Each tube containing 200 μM dNTPs, 0.2 μM of forward and reverse primers, 2 mM $MgCl_2$, 2 units of Taq polymerase and 1x Taq buffer. The forward primer: (5′- ATACCAGCTTATTCAATT-3′) used is coupled with a fluorophore label, Flu (fluorescein), to perform fluorescence measurements after each round to compare the aptamer enrichments from each cycle. On the other hand, the reverse primer (5′-poly-dA_{20}-HEGL-AGATTGCACTTACTATCT-3′) is coupled with a hexa-ethylene glycol linker extended with a poly-A_{20} chain. PCR conditions were as follows: 10 min at 94 °C, subsequently moving to 25 cycles of 94 °C for 1 min, 47 °C for 1 min, 72 °C for 1 min, and a final extension step at 72 °C for 10 min. Ethanol precipitation was carried out to concentrate/reduce the volume of the PCR product. 0.1 volume of 3 M sodium acetate followed by 3 vol of chilled 100% ethanol were added to the PCR product and this mixture was thoroughly vortexed. Next, the sample was kept at −80 °C for an hour and then centrifuged for 30 min at 13,000×*g* (4 °C). The pellet obtained after centrifugation was washed with 75% cold ethanol and dried at 90 °C for 3–5 min to eliminate any ethanol traces. The pellet was suspended in water and formamide solution (1:2 v/v) and then heated at 90 °C for 10 min. The concentrated PCR product was subjected to 12% denaturating polyacrylamide gel electrophoresis (PAGE) to separate the desired ssDNA aptamer from the dsDNA (PCR product). Due to the molecular mass differences in the two strands of the dsDNA, the fluorescein-labeled low mass ssDNA migrate faster than the higher mass ssDNA containing poly-dA_{20}-HEGL. After completion of the electrophoresis, the fluorescent bands were cut out, crushed, and added to the TE buffer solution. The crushed gel and the TE buffer mixture was chilled for 30 min at $-80°C$ and subsequently heated for 30 min at 90 °C. It was kept rotating overnight at 37 °C to elute the ssDNA from the gel. The eluted ssDNA from the TE buffer was concentrated, desalted with water using an ultrafiltration device, quantified by UV, and then used as ssDNA pool for the next round of selection.

2.5. Cloning and sequencing

The fluorescence intensity values indicate that the aptamer's recovery begins to plateau after12 rounds of SELEX. The target bound ssDNA eluted from the last round was PCR amplified using unmodified forward and reverse primers. The double-stranded PCR product was ligated with the pCR2.1-TOPO vector using the TOPO TA kit according to the manufacturer's protocol. The ligated circular product was transformed into *E. coli* DH5α competent cells by heat shock at 42 °C and cool down to ice temperature. The heat-treated E. coli cells were transformed to the pre-warmed Super Optimal broth with Catabolite repression(SOC) medium and incubated with shaking for an hour at 37 °C. Variable concentrations of the cells were spread on the Lauria Broth (LB) agar plate containing ampicillin and X-Gal. White and blue colonies were developed after overnight incubation at 37 °C. The positive white colonies were picked and the ssDNA aptamer inserts were amplified by colony PCR using M13 forward and reverse primers. The insertion of the aptamers sequences was confirmed by the presence of 300 bp using 2% agarose gel electrophoresis. The colony PCR product was sequenced and aligned by using *PRALINE* program.

2.6. Determination of dissociation constant of BC and OC aptamers

The selected aptamer sequences were chemically synthesized with fluorescein label for the determination of affinity constant (K_d). The affinity of each aptamer was determined by binding assays. In brief, different concentrations of the labeled aptamers in the binding buffer were heated to 90 °C for 10 min, 4 °C for 10 min and then 25 °C for 5 min. Each heat-treated aptamers were incubated with a constant volume of BC or OC conjugated sepharose beads for 1 h. Next, the beads were washed with binding buffer until there was no fluorescence from the washing. The target bound DNA aptamers were eluted using elution buffer. The amount of DNA recovered from the elution was reflected in the fluorescence intensity. The ssDNA input concentration was plotted against the fluorescence intensity. Saturation curves were obtained for each aptamer sequence, as shown in the (Fig. 2A and B). The dissociation constants were calculated by fitting the curve with nonlinear regression analysis using Prism software.

2.7. Graphene oxide-based fluorescence assay for OC and BC detection

Graphene oxide (GO) is used as a sensing platform for the detection of BC and OC by fluorescence assay. The amount of labeled aptamer used in this study was optimized based on the measurable fluorescence signals with a significant signal to noise ratio in the presence of GO. The optimal GO to aptamer ratio was optimized by titrating the different concentration GO (rage of 0–50 μg/m) with a fixed concentration of the labeled aptamer. From the fluorescence intensity, the concentration of the aptamer was optimized to 25 nM. After the addition of GO to the 25 nM of fluorescent aptamer, the solution was incubated for about 30 min for the maximum adsorption of the DNA aptamer on the graphene oxide sheet surface. The dynamic range of 0–150 pg/ml of the OC or BC was incubated with the GO-aptamer mixture (15 μg/ml-25 nM) for about 30–35 min in binding buffer. The fluorescence of each sample was measured with the excitation and emission wavelengths of 470 ± 10 nm and 515 nm, respectively. The fluorescence intensities of each sample were plotted against the corresponding concentrations of the BC or OC used.

2.8. Cross-reactivity and real sample analysis

The GO-based aptamer sensor was incubated with specific concentrations of different kinds of non-specific proteins such as bovine serum albumin (BSA) and Tropomyosin(TPM). After 30 min of incubation, the fluorescence was measured for each sample to find the cross-reacting protein with the sensors. For the BC aptasensor, OC was used as one of the non-specific protein and vice versa. To validate the sensors, we spiked the known concentrations of BC and OC in PBS buffer and incubated with the respective sensors for an hour. The changes in the fluorescence signals were used to calculate the percentage of recovery from the standard plot. The serum samples from the healthy and osteoporotic rats were diluted 100 times in binding buffer and mixed with the sensor. After 30 min of incubation, the fluorescence of each sample was measured. The osteoporosis rat model was developed after long-term treatment with a glucocorticoid drug (Dexamethasone) as reported in another study [35]. The animal study was carried out according to a protocol approved by the animal care and use committee (ACUC) at KFSHRC (RAC# 2150016).

3. Results and discussion

3.1. Immobilization of BC and OC on the sepharose beads surface

OC and BC are an essential bone formation biomarkers for bone formation and resorption used mainly for osteoporosis therapeutic monitoring and diagnosis. Developing biosensors for detecting BC and OC is very crucial, where we selected the specific aptamers for these target molecules. In the SELEX processes, the target molecules were immobilized using solid support to be used for the separation of bound and free ssDNA. Carboxylic acid-functionalized sepharose beads were activated with N- Hydroxysuccnimide (NHS), which can react with a free amine group in the target molecules in an aqueous medium without affecting any other functional groups [26]. The target molecules, BC and OC proteins, have free amine groups that can react with NHS activated sepharose beads and covalently linked in the presence of amine-free buffer (bicarbonate pH = 8.3) at the slightly basic condition. The reaction was carried out at 4 °C to maintain the functional properties of the target molecules. The non-reacted active sites with the NHS group were blocked with Tris-HCl to avoid any non-specific adsorption of ssDNA molecules during the SELEX process.

3.2. Selection of specific aptamers for BC and OC

The in vitro selection of a specific aptamer is mainly achieved in multiple steps, as shown in the Scheme- S1. In the first step, a pool of ssDNA library with 2×10^{15} sequences, consist of 60 random nucleotides and 18 fixed primer binding sites in both 3′ and 5’ ends, was incubated with target molecules conjugated to the beads (positive conjugation). The second step is the unbound ssDNA removal by washing the beads with an excess amount of binding buffer. In the third step, the high-affinity target-ssDNA complex was eluted using the elution buffer, desalted, and DNA amplification of bound DNA using PCR (Scheme- S1). The last step is the separation of the complementary aptamer ssDNA strand and PAGE purification of ssDNA. After seven cycles of SELEX, blank beads were incubated with a pool of ssDNA to remove the non-specific ssDNA, which binds to the sepharose beads, the spacer between the beads and the target molecules [33].

Fluorescein-labeled forward primer was used in the PCR amplification, which will be the ssDNA aptamer after PCR amplification, followed by strand separation and purification. The enrichment in the target bound ssDNA sequences was monitored by increasing the fluorescence signal from each round. In general, there may not be a significant fluorescence signal for the first few rounds. Therefore, we did not measure the fluorescence for the first four rounds of SELEX. We followed the ssDNS recovery and fluorescence enrichment from the 5^{th} round of OC and BC, respectively. As shown in Fig. 1A, and Fig. 1B, the fluorescence signal increases for each successive round, and significant enrichment was observed in the seventh round. After counter selection with the blank beads, a significant decrease in the fluorescence was observed in the eighth round of SELEX in both analytes due to the elimination of non-specific aptamer bound to the sepharose beads. The fluorescence recovery was increased after subsequent rounds, indicating that the enrichment in the high-affinity aptamer pool with the increase in the number of SELEX rounds. The SELEX process was quenched after a minimal increase in the fluorescence recovery in the 12^{th} round. The last round ssDNA was amplified and cloned in the *E. coli* DH5α competent cells. After overnight incubation at 37 °C, about 25 white colonies were picked up followed by colony PCR and sequencing. The extracted sequences were analyzed by the multiple sequence alignment program PRALINE (Fig. S1).

3.3. Determination of the dissociation constants (K_d) of aptamers

The binding affinity of the aptamer for the respective target molecules was studied by fluorescence-based assay. The sequences resulted from the cloning for OC were grouped, and four different aptamers (OC2, OC10, OC12, and OC17) were selected for dissociation constant (K_d) measurements. For BC, two aptamers (BC1 and BC2) were selected for the determination of K_d values. These measurements have been performed by incubating a fixed amount of a positive target (BC or OC) beads with different concentrations of fluorescently labeled aptamers in the dynamic range of 0–300 nM. The unbound aptamers were removed by washing with binding buffer after 1 h of incubation. The BC and OC

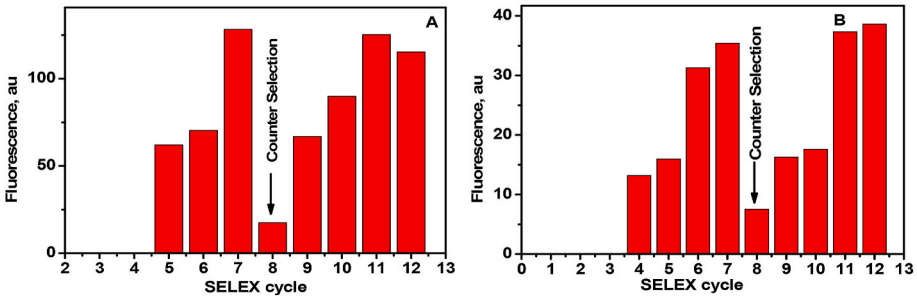

Fig. 1. Enhancement of beta-crosslaps (A) and osteocalcin (B)specific aptamers in the successive steps of SELEX procedure. (A) The bar graphs represent the fluorescence intensity of the bound ssDNA eluted from BC conjugated sepharose beads in each round. The sepharose bound ssDNA was eliminated by counter selection (CS) at the 8th cycle. (B)) The bar graphs represent the fluorescence intensity of the bound ssDNA eluted from OC conjugated sepharose beads in each round. The sepharose bound ssDNA was eliminated by counter selection (CS) at the 8th cycle.

bound ssDNA aptamers were eluted using hot elution buffer. The fluorescence intensities of samples were measured and plotted against their respective ssDNA. The K_d of each aptamer was obtained by fitting the saturation curve using non-linear regression analysis(Fig. 2A and Fig. 2B). The BC1 and BC2 aptamers show high affinity in the nanomolar range, 69 and 59 nM, respectively (Table-S1). The four aptamers selected for OC analytes show K_d values in the range 50–150 nM (Table-S1). As BC1 has a slightly higher K_d value, it was considered to be used for further studies due to the best fitting and less standard deviation in the K_d values. In the case of OC aptamer, OC2 was used for further studies due to its high-affinity.

3.4. Graphene oxide-based ON/OFF fluorescence assay

Unlike small molecule, protein and whole-cell targets are working very well with Graphene oxide-based fluorescence assay, in which a simple fluorescence on/off strategy is involved. The high-affinity aptamer for each analyte was used to construct aptasensors for the detection of BC and OC. As depicted in the Scheme-1, when the fluorescent-labeled aptamer is incubated with GO sheet, the aptamers are adsorbed on the GO surface by π stacking interactions between π electrons in GO and nucleotide bases in the ssDNA backbone. This interaction results in complete quenching of fluorescence due to fluorescence resonance energy transfer (FRET) from fluorescein to GO (off state), Scheme-1B. When the target molecule is introduced into the aptamer-GO complex, the aptamer gets detached from the GO surface due to its high affinity for the target. Therefore, in the presence of a target molecule, the fluorescence intensity increases rapidly (on the state) Scheme-1C.

3.5. Optimization of graphene oxide/aptamer ratio for fixing the off state of the sensor

The amount of GO required for maximum quenching of the fluorescent aptamer was determined by incubating different concentrations of GO with a fixed concentration of the fluorescently labeled aptamers. Fluorescent labeled BC1 and OC2 ssDNA aptamers were used for the optimization experiments, in which 25 nM aptamer was titrated against various concentrations of GO ranging from 0 to 50 μg/ml. In the absence of GO, a strong fluorescence of the fluorescein-labeled aptamer was observed. While the addition of GO with increasing concentrations, the fluorescence intensity was quenched rapidly as shown in Figs. 3A and 4A. More than 80% of the fluorescence was quenched, as the concentration of GO reached 20 μg/ml (Figs. 3B and 4B). There was no significant decrease in the fluorescence intensity by increasing the concentration of GO further. This was considered as the optimal off state with the minimal fluorescent signal. From the above results, the GO to BC1 or OC2 aptamer optimal ratio was fixed to be 20 μg/ml GO for 25 nM aptamer.

3.6. Detection of BC and OC using GO-based fluorescence assay

The ideal concentration ratio of GO and aptamer was used for detecting the BC and OC proteins. In the off state, more than 80% fluorescence of the fluorescein-labeled BC1 and OC2 were quenched as shown in Figs. 5A and 6A, respectively. Upon addition of proteins, the fluorescence of the aptamer recovered gradually with increasing concentration of BC or OC in the range of 0–144 pg/ml and 0–100 pg/ml for BC and OC, respectively, as shown in Figs. 5A and 6A. The calibration plots were obtained by plotting the percentage change in the fluorescence intensity versus the respective concentrations of the BC or OC as shown in Figs. 5B and 6B respectively. The limit of detections (LOD) of both aptasensors was calculated to be 0.21 pg/ml and 0.4 pg/ml for BC and OC, respectively. LOD was calculated from the standard deviation of the aptasensor signal in the absence of the analytes and the slope (m) obtained from the linear calibration plot using 3STD/m. The results showed that the GO-based fluorescence assay is highly sensitive and can detect BC and OC with the sub-picogram levels in the solution. The serum, OC levels of the healthy rats have been reported in the range of 0.6–1.66 ng/ml [36,37]. Other research groups have reported different levels of serum OC levels of unhealthy rats in the range from 50 to 180 ng/ml [38,39]. Ramanathan et al. have developed an electrochemical impedance spectroscopic immunosensor using an array of gold-coated vertically aligned carbon-nanotube(VACNT) electrodes for the label-free detection of bone resorption biomarker C-terminal telopeptide (cTx). The cTx antibody was immobilized on the gold modified CNT electrodes which favors the fabrication of the sensitive cTx immunosensor with the limit of detection 0.05 ng/ml [40]. An electrochemical

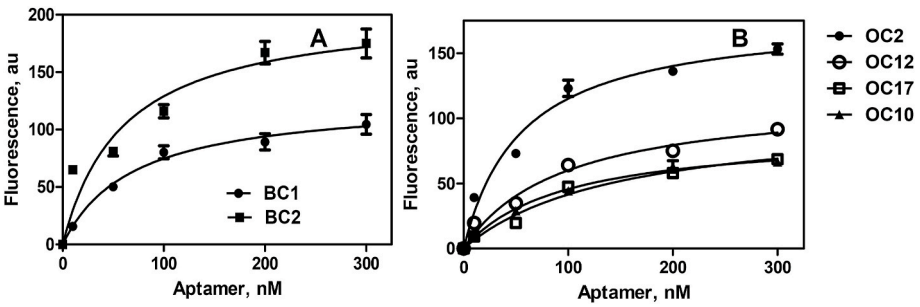

Fig. 2. Determination of affinity/dissociation constant (K_d) of from the saturation binding curve.

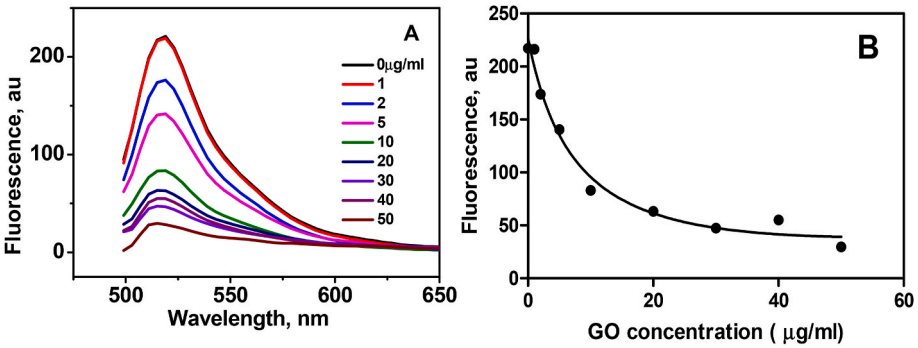

Fig. 3. (A) Fluorescence intensity of BC1 (25 nM) with increasing concentration of graphene oxide (GO (B) Plot GOconcentration vs fluorescence intensity of BC1 at 515 nm (λ-max). The fluorescence spectra were recorded by exciting at 470 ± 10 nm and the emission intensity 515 nm was used for the plots. The error bars represent the standard deviation of three different measurements.

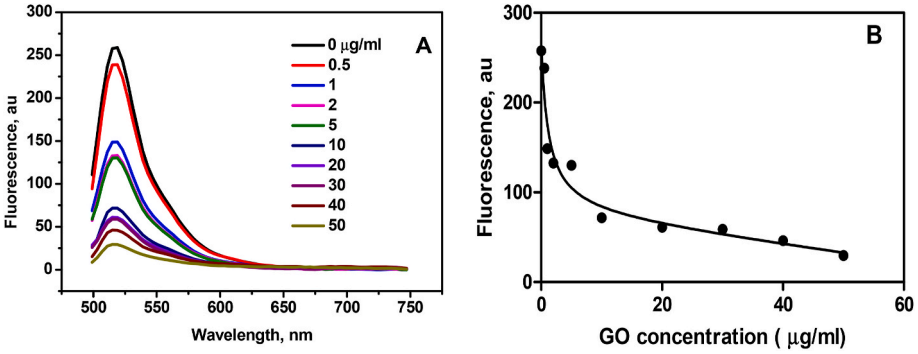

Fig. 4. (A) Fluorescence intensity of OC2 (25 nM) with increasing concentration of graphene oxide (GO) (B) Plot GO concentration vs fluorescence intensity of OC2 at 515 nm (λ-max). The fluorescence spectra were recorded by exciting at 470 ± 10 nm and the emission intensity 515 nm was used for the plots. The error bars represent the standard deviation of three different measurements.

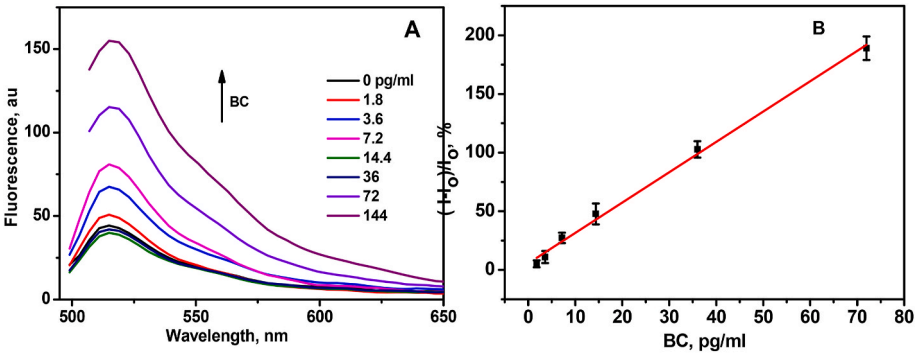

Fig. 5. (A) Aptamer (BC1) release from the GO surface by the addition of BC. Increase in the fluorescence intensity with increase in the concentration of protein. (B) The calibration plot fluorescence intensity against BC concentration (μg/mL) of BC1 at 515 nm. The fluorescence spectra were recorded by exciting at 470 ± 10 nm and the emission intensity 515 nm was used for the plots. The error bars represent the standard deviation of three different measurements.

biosensor has been developed for the sensing application of osteocalcin using the gold nanoparticle(GNps) modified gold electrode. The OC specific antibody was immobilized on the surface of the GNPs using L-glutathione and sulpho-NHS as coupling agents. The sensitivity of the immunosensor was 0.65 ng/ml [41]. Another group has developed an electrochemical immunosensor using an anti-osteocalcin antibody which is covalently immobilized on the gold electrode surface using 6-mercaptohexanol, 1,4-butanedioldiglycidyl ether, ethanolamine, and glutaraldehyde as coupling agents for the fabrication of self-assembled monolayer (SAM) based immunosensor with the sensitivity of 1.1 ng/ml [42]. Claudon et al. have fabricated an automated multiplex assay for the sensitive detection of four different born turnover biomarkers for osteoporosis diagnostic. The fully automated protein array chip could detect serum C-terminal cross-linked telopeptide of type I collagen (CTX-I), N-terminal propeptide of type I collagen (PINP), osteocalcin (OC) and intact parathyroid hormone(PTH) biomarkers in 20 in μl of serum simultaneously. The sensitivity of multiplex assay for each biomarker was 0.002 ng/ml, 0.26 ng/ml, 0.51 ng/ml, and 0.39 ng/ml for serum CTX-I, PINP, OC, and PTH, respectively [43]. Another multiplex assay platform was used for the simultaneous detection of osteocalcin and collagen type 1 cross-linked C-telopeptide. The platform integrates microfluidic technology with electrochemical sensing which could detect the serum levels of different biomarkers. The corresponding antibodies of the antigens were functionalized to immobilize the micro-fabricated Au electrodes which lead to the signal change upon capturing the respective antigens. The limit of detection for osteocalcin

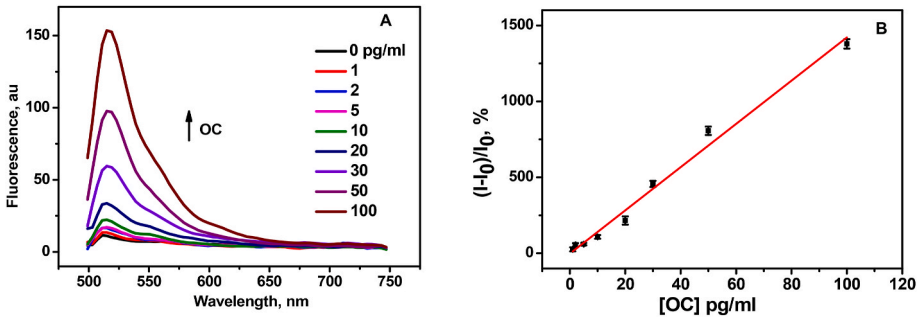

Fig. 6. (A) Aptamer (OC2) release from the GO surface by the addition of OC. Increase in the fluorescence intensity with increase in the concentration of protein. (B) The calibration plot fluorescence intensity against OC concentration (μg/mL) of OC2 at 515 nm. The fluorescence spectra were recorded by exciting at 470 ± 10 nm and the emission intensity 515 nm was used for the plots. The error bars represent the standard deviation of three different measurements.

and collagen type 1 cross-linked C-telopeptide were 1.94 ng/ml and 1.39 ng/ml respectively [44]. In comparison with the reported biosensors, Our results showed that the new aptamer-based detection method is much more rapid and highly sensitive to detect serum OC levels from both healthy and infected rats. The unhealthy rats have higher values of serum OC values compared to the healthy rats. The serum BC levels of the healthy rats have been reported as 7.0–7.5 ng/ml, whereas the infected rats have higher values compared to the intact one [45]. The high affinity of the aptamer and the optimized ideal sensor platform resulted in the fabrication of highly sensitive aptasensors.

3.7. Selectivity of the GO-aptasensor and application to real sample analysis

The specific binding of the fabricated aptasensors with BC was followed by testing the sensor with other related proteins such as BSA, tropomyosin, and OC. Similarly, OC specific aptasensor was tested with BSA, tropomyosin, and BC. There is no significant increase (10% or less) was observed in the fluorescence signal upon the addition of non-specific proteins, as shown in Fig. 7A and B. From the results, it is believed that simple GO-based fluorescence assay is selective and highly sensitive for the detection of BC or OC at deficient concentrations. Based on the performance of the BC1 and OC2 aptasensors, we validate their sensing ability of OC and BC in buffer spiked with respective analytes. The percentage recovery of analytes was compared with the standard calibration plot. As represented in the Table-S2, a good recovery percentage was obtained. Finally, we used the sensor to detect the amount of OC and BC in serum from the healthy rats using this sensor. The amount of serum OC and BC are found to be 151 ng/ml and 528 ng/ml from the healthy rats. We could not perform the OC and BC measurements without dilution, due to interference from autofluorescence and scattering from the biomolecules in the serum. Recently, Malkawi et al. have reported the OC and BC in serums levels of untreated rats as 140 and 500 ng/ml respectively using ELISA [35], which are close to our values obtained from the new aptasensors. From the results, we are confident that the sensor can be used for the real sample analysis. Though it is a sensitive method for monitoring the real sample, it has certain limitations. Nevertheless, the lack of homogeneity and transparency of clinical samples necessitates their proper dilution before their fluorescence intensities are monitored.

4. Conclusions

ssDNA specific aptamers for rat-osteocalcin and rat beta-crosslaps were selected by the SELEX technique for the first time. The target molecules were immobilized on the sepharose beads as solid support. The enrichment in the ssDNA aptamer binding to the target was monitored by an increase in the fluorescence intensity. The selected aptamers from the last round were cloned and sequenced. The high-affinity aptamers were identified by their K_d values (50–150 nM). The high-affinity aptamers for each analyte were used to fabricate the graphene oxide-based fluorescence assay for the sensitive detection of BC or OC. The assay is highly sensitive which can detect OC and BC in the picogram range. This assay can selectively detect the target molecules against other non-specific proteins. This simple fluorescence assay is potentially applicable for the rapid detection of BC and OC biomarkers osteoporosis and bone resorption cases.

Authors credits

Raja Chinnappan, Norhan Sameh Zaghloul, Razan AlZabn did most of the experimental work. Abeer Malkawi developed the animal model. Raja Chinnappan drafted the manuscript. Anas Abdel Rahman and Khalid Abu Salah proofed reading. Mohammed Zourob supervised the work.

Declaration of competing interest

The authors declare that they have no known competing financial interests or personal relationships that could have appeared to influence the work reported in this paper.

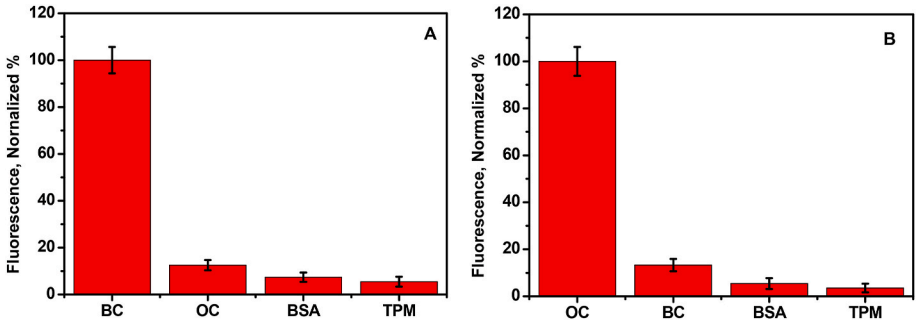

Fig. 7. The cross-reactivity response of GO- BC1 aptamer and GO- OC2 aptamer (20 μg/ml-25 nM). The fluorescence assays GO-BC1 aptasensor with BC and other irrelevant samples OC, BSA, and tropomyosin(A). The fluorescence assays GO-OC2 aptasensor with OC and other irrelevant samples BC, BSA and tropomyosin(B) The fluorescence intensity of each sample obtained by exciting at 470 ± 10 nm and the emission intensity 515 nm was used for the plots. The error bars represent the standard deviation of three different measurements.

Appendix A. Supplementary data

Supplementary data to this article can be found online at https://doi.org/10.1016/j.talanta.2020.121818.

Obtained from the titration of fluorescein-labeled aptamers and scrambled ssDNA with constant amount *BC* conjugated sepharose beads (A) and OC conjugated sepharose beads(B). The fluorescence spectra were recorded by exciting at 470 ± 10 nm and the emission intensity (515 nm) was used for the plots. The dissociation constants were calculated by nonlinear regression analysis. The error bars represent the standard deviation of three different measurements.

References

[1] H. Lv, F. Jiang, D. Guan, C. Lu, B. Guo, C. Chan, S. Peng, B. Liu, W. Guo, H. Zhu, X. Xu, A. Lu, G. Zhang, Metabolomics and its application in the development of discovering biomarkers for osteoporosis research, Int. J. Mol. Sci. 17 (2016) 17, https://doi.org/10.3390/ijms17122018, 2018.

[2] P. Kuru, G. Akyüz, H.P. Cerşit, A.E. Çelenlioğlu, A. Cumhur, Ş. Biricik, S. Kozan, A. Gökşen, M. Özdemir, E. Lüleci, Fracture history in osteoporosis: risk factors and its effect on quality of life, Balkan Med. J. 31 (2014) 295–301.

[3] N. Harvey, E. Dennison, C. Cooper, Osteoporosis: impact on health and economics, Nat. Rev. Rheumatol. 6 (2010) 99–105.

[4] S. Yang, Y. Liu, Q. Shi, J. Zou, H. Yang, Characteristics of bone biochemical indices in predicting secondary osteoporotic fracture after intertrochanteric fracture in elderly women, J. Orthop. Translat 12 (2018) 1–5.

[5] N.M. Al-Daghri, S. Yakout, E. Al-Shehri, H. Al-Fawaz, N. Aljohani, Y. Al-Saleh, Inflammatory and bone turnover markers in relation to PTH and vitamin D status among Saudi postmenopausal women with and without osteoporosis, Int. J. Clin. Exp. Med. 7 (2014) 2812–2819.

[6] D. Bubshait, M. Sadat-Ali, Economic implications of osteoporosis-related femoral fractures in Saudi Arabian society, Calcif. Tissue Int. 81 (2007) 455–458.

[7] K.M. Prestwood, L.G. Raisz, Prevention and treatment of osteoporosis, Clin. Cornerstone 2 (2000) 34–44.

[8] Y.Z. Pi, X.P. Wu, S.P. Liu, X.H. Luo, X.Z. Cao, H. Xie, E.Y. Liao, Age-related changes in bone biochemical markers and their relationship with bone mineral density in normal Chinese women, J. Bone Miner. Metabol. 24 (2006) 380–385.

[9] A. Saller, S. Maggi, G. Romanato, P. Tonin, G. Crepaldi, Diabetes and osteoporosis, Aging Clin. Exp. Res. 20 (2008) 280–289.

[10] E. Bidoli, D. Schinella, S. Franceschi, Physical activity and bone mineral density in Italian middle-aged women, Eur. J. Epidemiol. 14 (1998) 153–157.

[11] H. Johansson, J.A. Kanis, A. Oden, E. McCloskey, R.D. Chapurlat, C. Christiansen, S.R. Cummings, A. Diez-Perez, J.A. Eisman, S. Fujiwara, C.C. Gluer, D. Goltzman, D. Hans, K.T. Khaw, M.A. Krieg, H. Kroger, A.Z. LaCroix, E. Lau, W.D. Leslie, D. Mellstrom, L.J. Melton 3rd, T.W. O'Neill, J.A. Pasco, J.C. Prior, D.M. Reid, F. Rivadeneira, T. van Staa, N. Yoshimura, M.C. Zillikens, A meta-analysis of the association of fracture risk and body mass index in women, J. Bone Miner. Res. 29 (2014) 223–233.

[12] P.D. Delmas, R. Rizzoli, C. Cooper, J.Y. Reginster, Treatment of patients with postmenopausal osteoporosis is worthwhile. The position of the International Osteoporosis Foundation, Osteoporos. Int. 16 (2005) 1–5.

[13] M.H. Knapen, L.J. Schurgers, C. Vermeer, Vitamin K2 supplementation improves hip bone geometry and bone strength indices in postmenopausal women, Osteoporos. Int. 18 (2007) 963–972.

[14] K. Panday, A. Gona, M.B. Humphrey, Medication-induced osteoporosis: screening and treatment strategies, Ther. Adv. Musculoskelet Dis. 6 (2014) 185–202.

[15] J.P. Brown, P.D. Delmas, L. Malaval, C. Edouard, M.C. Chapuy, P.J. Meunier, Serum bone Gla-protein: a specific marker for bone formation in postmenopausal osteoporosis, Lancet 1 (1984) 1091–1093.

[16] K. Mukaiyama, M. Kamimura, S. Uchiyama, S. Ikegami, Y. Nakamura, H. Kato, Elevation of serum alkaline phosphatase (ALP) level in postmenopausal women is caused by high bone turnover, Aging Clin. Exp. Res. 27 (2015) 413–418.

[17] M.M. Brzoska, J. Moniuszko-Jakoniuk, Low-level lifetime exposure to cadmium decreases skeletal mineralization and enhances bone loss in aged rats, Bone 35 (2004) 1180–1191.

[18] X. Liu, S. Zhang, X. Lu, S. Zheng, F. Li, Z. Xiong, Metabonomic study on the anti-osteoporosis effect of Rhizoma Drynariae and its action mechanism using ultra-performance liquid chromatography-tandem mass spectrometry, J. Ethnopharmacol. 139 (2012) 311–317.

[19] H. Reichel, H.J. Roth, H. Schmidt-Gayk, Evaluation of serum beta-carboxy-terminal cross-linking telopeptide of type I collagen as marker of bone resorption in chronic hemodialysis patients, Nephron. Clin. practice 98 (2004) c112–118.

[20] T.P. Cleland, C.J. Thomas, C.M. Gundberg, D. Vashishth, Influence of carboxylation on osteocalcin detection by mass spectrometry, Rapid Commun. Mass Spectrom. 30 (2016), 2109-2015.

[21] F. Rahimi, J. Mohammadnejad Arough, M. Yaghoobi, H. Davoodi, F. Sepehri, M. Amirabadizadeh, A novel approach for osteocalcin detection by competitive ELISA using porous silicon as a substrate, Biotechnol. Appl. Biochem. 64 (2017) 871–878.

[22] M. Ferron, J. Wei, T. Yoshizawa, P. Ducy, G. Karsenty, An ELISA-based method to quantify osteocalcin carboxylation in mice, Biochem. Biophys. Res. Commun. 397 (2010) 691–696.

[23] R. Okabe, M. Inaba, K. Nakatsuka, T. Miki, H. Naka, A. Moriguchi, Y. Nishizawa, Significance of serum CrossLaps as a predictor of changes in bone mineral density during estrogen replacement therapy; comparison with serum carboxyterminal telopeptide of type I collagen and urinary deoxypyridinoline, J. Bone Miner. Metabol. 22 (2004) 127–131.

[24] C. Rosenquist, C. Fledelius, S. Christgau, B.J. Pedersen, M. Bonde, P. Qvist, C. Christiansen, Serum CrossLaps One Step ELISA. First application of monoclonal antibodies for measurement in serum of bone-related degradation products from C-terminal telopeptides of type I collagen, Clin. Chem. 44 (1998) 2281–2289.

[25] J.A. Calero, M.T. Munoz, J. Argente, M.L. Traba, C. Mendez-Davila, C. Garcia-Moreno, C. de la Piedra, A variation in Bone Alkaline Phosphatase levels that correlates positively with bone loss and normal levels of aminoterminal propeptide of collagen I in girls with anorexia nervosa, Clin. Chim. Acta 285 (1999) 121–129.

[26] M.M. Aljohani, R. Chinnappan, S. Eissa, O.A. Alsager, K. Weber, D. Cialla-May, J. Popp, M. Zourob, In vitro selection of specific DNA aptamers against the anti-coagulant dabigatran etexilate, Sci. Rep. 8 (2018) 13290, https://doi.org/10.1038/s41598-018-31327-3.

[27] R. Chinnappan, R. AlZabn, K.M. Abu-Salah, M. Zourob, An aptamer based fluorometric microcystin-LR assay using DNA strand-based competitive displacement, Microchim. Acta. 186 (2019) 435, https://doi.org/10.1007/s00604-019-3504-8.

[28] S. Eissa, A. Siddiqua, R. Chinnappan, M.M. Zourob, Electrochemical SELEX technique for the selection of DNA aptamers against the small molecule 11-deoxycortisol, ACS Appl. Bio Materials (2019) 2624–2632.

[29] R. Chinnappan, S. Eissa, A. Alotaibi, A. Siddiqua, O.A. Alsager, M. Zourob, In vitro selection of DNA aptamers and their integration in a competitive voltammetric biosensor for azlocillin determination in waste water, Anal. Chim. Acta 1101 (2019) 149–156.

[30] R. Chinnappan, S. AlAmer, S. Eissa, A.A. Rahamn, K.M.A. Salah, M. Zourob, Fluorometric graphene oxide-based detection of Salmonella enteritis using a truncated DNA aptamer, Microchim. Act 185 (2018) 61, https://doi.org/10.1007/s00604-017-2601-9.

[31] R. Chinnappan, A.A. Rahamn, R. AlZabn, S. Kamath, A.L. Lopata, K.M. Abu-Salah, M. Zourob, Aptameric biosensor for the sensitive detection of major shrimp allergen, tropomyosin, Food Chem. (2019) 126133, https://doi.org/10.1016/j.foodchem.2019.126133.

[32] R. Chinnappan, R. AlZabn, T.A. Mir, M. Bader, M. Zourob, Fluorometric determination of okadaic acid using a truncated aptamer, Microchim. Act 186 (2019) 406, https://doi.org/10.1007/s00604-019-3517-3.

[33] S. Eissa, S. Alkhaldi, R. Chinnappan, A. Siddiqua, M. Abduljabbar, A.M.A. Rahman, M. Dasouki, M. Zourob, Selection, Characterization, and Electrochemical Biosensing Application of DNA Aptamers for Sepiapterin, Talanta, 2020, p. 120951, https://doi.org/10.1016/j.talanta.2020.120951.

[34] R. Chinnappan, R. AlZabn, A.K. Fataftah, A. Alhoshani, M. Zourob, Probing high-affinity aptamer binding region and development of aptasensor platform for the detection of cylindrospermopsin, Anal. Bioanal. Chem. 412 (2020) 4691–4701.

[35] A.K. Malkawi, K.H. Alzoubi, M. Jacob, G. Matic, A. Ali, A. Al Faraj, F. Almuhanna, M. Dasouki, A.M. Abdel Rahman, Metabolomics based profiling of dexamethasone side effects in rats, Front. Pharmacol. 9 (2018) 46, https://doi.org/10.3389/fphar.2018.00046.

[36] H.M. Kir, S. Garip, D. Sahin, B. Öztaş, Effects of carbamazepine on serum parathormone, 25- hydroxyvitamin D, bone specific alkaline phosphatase, C-telopeptide, and osteocalcin levels in healthy rats, Bosn. J. Basic Med. Sci. 12 (2012) 240–244.

[37] C. Ce, L. Zhou, D. Yu, Y. Zhao, N. Yang, Serum osteocalcin levels and bone mineral density in ovariectomized rats, Int. J. Innov. Sci. Res. 5 (2014) 1–8.

[38] H. Tanaka, H. Shirota, M. Kuwada, K. Terato, K. Katayama, Plasma and bone osteocalcin levels in rats with type ii collagen—induced arthritis, Arthritis Rheum.: Off. J. Am. Colleg.Rheumat. 31 (1988) 1413–1420.

[39] D. Lim, Y. Kim, Anti-osteoporotic effects of Angelica sinensis (Oliv.) Diels extract on ovariectomized rats and its oral toxicity in rats, Nutrients 6 (2014) 4362–4372.

[40] M. Ramanathan, M. Patil, R. Epur, Y. Yun, V. Shanov, M. Schulz, W.R. Heineman, M.K. Datta, P.N. Kumta, Gold-coated carbon nanotube electrode arrays: immunosensors for impedimetric detection of bone biomarkers, Biosens. Bioelectron. 77 (2016) 580–588.

[41] P. Khashayar, G. Amoabediny, M. Hosseini, R. Verplancke, F. Razi, J. Vanfleteren, B. Larijani, An electrochemical biosensor based on AuNP-modified gold electrodes for selective determination of serum levels of osteocalcin, IEEE Sensor. J. 17 (2017) 3367–3374.

[42] S.I. Kabala, H. Yagar H.M. Ozcan, A new biosensor for osteoporosis detection, Prep. Biochem. Biotechnol. 49 (2019) 511–520.

[43] A. Claudon, P. Vergnaud C. Valverde, A. Mayr, U. Klause, P. Garnero, New automated multiplex assay for bone turnover markers in osteoporosis, Clin. Chem. 54 (2008) 1554–1563.

[44] P. Khashayar, G. Amoabediny, B. Larijani, M. Hosseini, R. Verplancke, D. Schaubroeck, S.V. Put, F. Razi, M.D. Keersmaecker, A. Adriaens, S. Goemaere, T. Fiers, J. Vanfleteren, A multiplexed microfluidic platform for bone marker measurement: a proof-of-concept, Micromachines 8 (2017) 133, https://doi.org/10.3390/mi8050133.

[45] D.B. Hoffmann, J. Gruber, K.O. Böker, D. Deppe, S. Sehmisch, A.F. Schilling, N. Lemus-Diaz, M. Komrakova, S. Schneider, Effects of RANKL knockdown by virus-like particle-mediated RNAi in a rat model of osteoporosis, Mol. Ther. Nucleic Acids 12 (2018) 443–452.